

Peierls distorted chain as a quantum data bus for quantum state transfer

M.X. Huo, Ying Li, and Z. Song*

Department of Physics, Nankai University, Tianjin 300071, China

C.P. Sun†

*Institute of Theoretical Physics, Chinese Academy of Sciences, Beijing, 100080, China and
Department of Physics, Nankai University, Tianjin 300071, China*

We systematically study the transfer of quantum state of electron spin as the flying qubit along a half-filled Peierls distorted tight-binding chain described by the Su-Schrieffer-Heeger (SSH) model, which behaves as a quantum data bus. This enables a novel physical mechanism for quantum communication with always-on interaction: the effective hopping of the spin carrier between sites A and B connected to two sites in this SSH chain can be induced by the quasi-excitations of the SSH model. As we prove, it is the Peierls energy gap of the SSH quasi-excitations that plays a crucial role to protect the robustness of the quantum state transfer process. Moreover, our observation also indicates that such a scheme can also be employed to explore the intrinsic property of the quantum system.

PACS numbers: 03.65.Ud, 03.67.MN, 71.10.FD

I. INTRODUCTION

In many protocols of quantum information processing, it is crucial to transmit the quantum state of qubits with high fidelity [1]. While various schemes of quantum state transfer (QST) were proposed and demonstrated experimentally [2] for the optical system even with atom ensemble [3, 4], people have tried the best to implement this task based on the solid-state systems, which are believed as the best candidates for the scalable quantum computing [5, 6]. It was recognized that the quantum spin chain [7, 8] and the Bloch electron system [9] with the artificial nearest neighbor (NN) couplings can be used as quantum data buses to transfer quantum information perfectly. In Ref. [8], we discovered that the spectrum-parity matching is responsible for the perfectness of most protocols of QST.

However, these solid-state based schemes for implementing quantum data bus are too artificial with very specially designed NN couplings and only single-particle cases were considered. Though it is believed that such an engineered quantum system will be realized in the future experiments, at least, this difficulty should be overcome in theoretical aspect. To this end, we have tried to employ the higher-dimensional system or the complicated quantum network, such as the spin ladder [10]. Though the spin ladder is not an ideal medium serving as a perfect data bus, it shows that the long-distance QST is possible via the multi-exciton system due to the existence of the spin gap, which is much larger than the coupling strength connecting two separated qubits to the two ends of the ladder respectively.

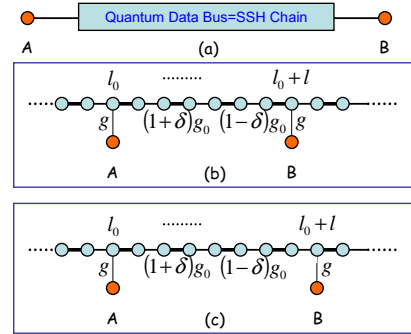


FIG. 1: (a) The schematic illustration of the system. Two sites A and B connect to the two sites of PDTBC with the distance l being (b) odd and (c) even.

A medium can be a robust quantum data bus if the fidelity of transferring a quantum state between two sites attached to it approaches unity at a finite temperature. These consideration motivates us to use more natural energy gapped materials to act as a quantum data bus. In this paper, we study the function of quantum data bus for the conducting polymers (polyacetylene), modeled as a Peierls distorted tight-binding chain (PDTBC) or the Su-Schrieffer-Heeger (SSH) model [11, 15]. It is well known that, taking the coupling between electron and photon into account, such a system exhibits an instability against the lattice distortion, which induces an energy gap for the spectrum in half-filled case as a result of dimerization. Therefore, the SSH chain is a good candidate of quantum data bus for fermion, which is just similar to the spin ladder for spin [10]. Furthermore, such a practical system allows us to investigate the case with larger particle number by performing analytical analysis for the two distant separated probe points AB since the SSH model can be solved exactly.

*Electronic address: songtc@nankai.edu.cn

†Electronic address: suncp@itp.ac.cn;
URL: <http://www.itp.ac.cn/~suncp>

As a protocol for the quantum communication with always-on interaction, two points A and B are connected to two sites of the SSH chain (see the Fig. 1(a)). For the half-filled case, when the connections of A and B with SSH chain are switched off, the ground states are two-fold degenerate due to the vanishing on-site chemical potential. When the connections switch on, the two degenerate levels split while the eigenstates remain nearly half-filled for the subsystem AB due to the energy gap of the SSH chain. It leads to the effective interaction between A and B . Thus the level spacing of two lowest eigenstates directly corresponds to the effective hopping integral between A and B and determines the validity of quantum state transfer via such a medium. Generally, if the energy gap is large enough, an effective Hamiltonian H_{AB} of these two sites is induced by this quantum data bus to perform perfect QST at low temperature. Thus the validity of H_{AB} and the behavior of the effective hopping integral (level spacing of two lowest eigenstates) as the distance between A and B increases are crucial for the quality of a quantum data bus. To demonstrate the properties of our scheme, we compare the eigenstates of H_{AB} with those reduced density matrices from the ground and the first excited states of the total system. We find that the Peierls energy gap of the SSH chain plays an important role in protecting the robustness of the QST. The main conclusions are achieved both with the analytical study and numerical calculation.

This paper is organized as follows. In Sec. II, the model setup of our protocol and the spectrum of SSH chain are introduced. As a reasonable approximation up to second order, the effective Hamiltonian H_{AB} with respect to the two separated points A and B is deduced by using the Fröhlich transformation [12, 13] to “remove” the degree of freedom of SSH model in Sec. III. In Sec. IV, the density matrices of qubits A and B for the ground and the first excited states of the whole system are calculated to demonstrate the quantum entanglement of them over a long distance. The QST scheme is also investigated numerically in the region of the crossover between two types of dimerization. It shows that, at this transition point, the QST becomes fastest, but with the similar lost of fidelity to what has been discussed in the Ref. [20]. In Sec. V, we discuss the quantum decoherence problem due to the quasi-excitations of the SSH chain at finite temperature. The summary and remarks are presented finally in Sec. VI.

II. MODEL SETUP OF QUANTUM DATA BUS BASED ON THE SSH CHAIN

In a polyacetylene, σ -electrons, which are localized between the two bonded nuclei, connect one C atom with the neighboring two C and one H atoms to form an elementary linear configuration; π -electrons, which are less localized, behave as Bloch electrons. Such a system can be treated by using tight-binding approximation and π -

electrons can be the candidate as a carrier of quantum information [9]. Here, we also consider the coupling between electrons and dispersionless phonons represented by local oscillators.

Let u_n be the displacement of the n th CH (the unit of a polyacetylene) from the equilibrium position. Then, the tight-binding Hamiltonian reads as

$$H_{SSH} = - \sum_{n,\sigma} g_{n+1} \left(c_{n+1,\sigma}^\dagger c_{n,\sigma} + h.c. \right) + H_C, \quad (1)$$

where

$$H_C = \sum_n \left[\frac{\Pi_n^2}{2M} + \frac{1}{2} K (u_{n+1} - u_n)^2 \right] \quad (2)$$

describes the lattice motion. Here, $g_{n+1} = g_0 - \lambda(u_{n+1} - u_n)$ is the hopping integral and λ is the electron-lattice coupling constant. Π_n denotes the canonical momentum operator conjugate to u_n and M is the effective mass of the unit of a polyacetylene (CH). K is the spring constant due to σ -electrons, and $c_{j,\sigma}$ ($c_{j,\sigma}^\dagger$) is annihilation (creation) operator of π -electrons on site j with spin $\sigma = \pm 1$. This Hamiltonian is proposed by Su, Schrieffer and Heeger [11] to describe the dimerization phenomenon of the polyacetylene in association with its conductivity.

In our scheme, we consider the QST between sites A and B connected to the two sites of the SSH chain. Our purpose is to transfer a qubit state, which is in a superposition state of electron spin up and spin down, through the hopping of an polarized electron from the site A to B (see the Fig. 1(b)). Since the Hamiltonian (1) does not contain spin dependent interaction, the spin polarization of every electron is conservative. In this sense, the spatial motion of electrons along the chain will carry a spin state from one location to another. Thus, we can study the fidelity of spin state transfer by considering the fidelity of charge state transfer. The connection of sites A and B to the SSH chain is described by the Hamiltonian

$$H_I = -g \sum_{\sigma} \left(c_{A,\sigma}^\dagger c_{l_0,\sigma} + c_{B,\sigma}^\dagger c_{l_0+l,\sigma} + h.c. \right), \quad (3)$$

where $c_{A,\sigma}$ and $c_{B,\sigma}$ ($c_{A,\sigma}^\dagger$ and $c_{B,\sigma}^\dagger$) are annihilation (creation) operators of electrons on sites A and B with spin σ , while l_0 and $l_0 + l$ denote the connecting sites in the SSH chain.

In Fig. 2, we intuitively demonstrate how the above Hamiltonian can lead to the effective hopping of electron between the additional sites A and B . We will also show how the effective hopping integral depends on the distance between them. The original energy degeneracy at $E = 0$ of the subsystem formed by A and B will be removed by the switching on g and then split into two sub-levels with the level spacing $2g_{eff}$. Here, g_{eff} is the effective hopping integral, which can be obtained analytically as follows.

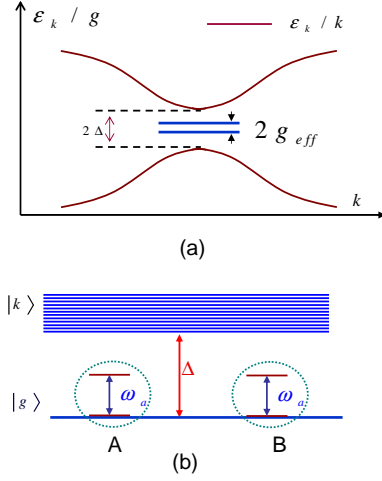


FIG. 2: (a) The single particle energy spectrum of dimerized polyacetylene. (b) The eigenstates of the effective Hamiltonian about points A and B.

To consider how a SSH chain can be used as a quantum data bus to transfer a quantum state, we first summarize the known results about diagonalization of the SSH Hamiltonian. The most important discovery is the prediction about the Peierls transition happens when the polyacetylene is dimerized as $u_n = (-1)^{n-1} u_0$. It minimizes the energy of the one-dimensional electronic gas when the lattice vibrates slowly so that the Born-Oppenheimer approximation can determine an instantaneous eigen energy of electron for a fixed lattice configuration. After dimerization, the Hamiltonian then reads

$$H_{SSH} = - \sum_{n,\sigma} g_0 [1 - (-1)^n \delta] (c_{n+1,\sigma}^\dagger c_{n,\sigma} + h.c.) + E_0, \quad (4)$$

where $\delta = 2\lambda u_0 / g_0$ denotes the distortion of the hopping integral and E_0 is a constant. Taking periodic boundary condition, it can be diagonalized as

$$H_{SSH} = \sum_{k,\sigma} \epsilon_k (\alpha_{k,\sigma}^\dagger \alpha_{k,\sigma} - \beta_{k,\sigma}^\dagger \beta_{k,\sigma}), \quad (5)$$

with the dispersion relation

$$\epsilon_k = 2g_0 \sqrt{\cos^2 \frac{k}{2} + \delta^2 \sin^2 \frac{k}{2}} \quad (6)$$

for the excitations described by the fermion operators

$$\alpha_{k,\sigma} = \frac{1}{\sqrt{N}} \sum_{j=1}^{N/2} e^{-ikj} (c_{2j-1,\sigma} - e^{i\theta_k} c_{2j,\sigma}) \quad (7)$$

and

$$\beta_{k,\sigma} = \frac{1}{\sqrt{N}} \sum_{j=1}^{N/2} e^{-ikj} (c_{2j-1,\sigma} + e^{i\theta_k} c_{2j,\sigma}), \quad (8)$$

where N is the number of CH in polyacetylene chain (or the length of the chain), $k = 4\pi m / N$, $m = 0, 1, 2, \dots, N/2 - 1$, and

$$e^{i\theta_k} = \frac{g_0}{\epsilon_k} [(1 + \delta) + (1 - \delta) e^{-ik}]. \quad (9)$$

The single-particle spectrum (6) is illustrated in the Fig. 2(a) and the energy gap between the two bands is

$$2\Delta = 2 \min \{\epsilon_k\} = 4g_0\delta. \quad (10)$$

In next section, we will show that such an energy gap is necessarily required for a desirable robust quantum data bus for QST. Usually, as illustrated in Fig. 2(b), the large energy gap above the lowest two levels can provide a kind of “quantum protect” for the QST via the virtual excitations of the quantum data bus, which induce a long range hopping of electron between sites A and B in the low temperature. The dense continuity of spectrum above the gap ensures that the strength of the effective hopping integral across A and B is so strong that the fast entanglement can be generated. In the following, we will demonstrate that such a dimerized gap plays a same role for QST as the spin gap in spin ladder [10].

III. EFFECTIVE LONG RANGE HOPPING INDUCED BY VIRTUAL QUASI-EXCITATIONS

To deduce the effective Hamiltonian about the indirect coupling between two attached sites A and B, we utilize the Fröhlich transformation, whose original approach was used successfully for the BCS theory of superconductivity. The effective Hamiltonian $H_{eff} = UH U^{-1}$ can be achieved by a unitary operator $U = \exp(-S)$, where H is the Hamiltonian of the total system with the perturbation decomposition

$$H = H_{SSH} + H_I. \quad (11)$$

In the second order perturbation theory, we require the anti-Hermitian operator S obeys

$$H_I + [H_{SSH}, S] = 0. \quad (12)$$

Thus the effective Hamiltonian can be approximated as

$$H_{eff} \cong H_{SSH} + \frac{1}{2} [H_I, S]. \quad (13)$$

There are two ways to connect the two sites A and B to the SSH chain, with (without) the mirror inversion symmetry as showed in Fig. 1(b) (Fig. 1(c)). Here, only the case with both l_0 and l being odd is discussed. The result can be used to all cases, because the system is invariant under exchanging A and B. As the solution of Eq. (12), S can be expressed explicitly as

$$S = -\frac{g}{\sqrt{N}} \sum_{k,\sigma} \frac{1}{\epsilon_k} \left[e^{ik\frac{l_0+1}{2}} c_{A,\sigma}^\dagger (\alpha_{k,\sigma} - \beta_{k,\sigma}) - e^{ik\frac{l_0+1}{2} - i\theta_k} c_{B,\sigma}^\dagger (\alpha_{k,\sigma} + \beta_{k,\sigma}) - h.c. \right], \quad (14)$$

which leads to the effective Hamiltonian

$$H_{eff} = H_{AB} + H_0 \quad (15)$$

with

$$[H_{AB}, H_0] = 0. \quad (16)$$

Here

$$H_{AB} = \sum_{\sigma} g_{eff} \left(c_{A,\sigma}^{\dagger} c_{B,\sigma} + c_{B,\sigma}^{\dagger} c_{A,\sigma} \right) \quad (17)$$

denotes the effective hopping of electron between A and B with the strength

$$g_{eff} = \frac{2g^2}{N} \sum_k \frac{e^{-ik\frac{l-1}{2} + i\theta_k}}{\epsilon_k}, \quad (18)$$

while

$$\begin{aligned} H_0 = & \sum_{k,\sigma} \epsilon_k \left(\alpha_{k,\sigma}^{\dagger} \alpha_{k,\sigma} - \beta_{k,\sigma}^{\dagger} \beta_{k,\sigma} \right) + \frac{g^2}{2N} \\ & \times \sum_{k,\sigma,k',\sigma'} \frac{1}{\epsilon_{k'}} \left[A(k,k') \left(\alpha_{k,\sigma}^{\dagger} \alpha_{k',\sigma'} - \beta_{k,\sigma}^{\dagger} \beta_{k',\sigma'} \right) \right. \\ & \left. + B(k,k') \left(\beta_{k,\sigma}^{\dagger} \alpha_{k',\sigma'} - \alpha_{k,\sigma}^{\dagger} \beta_{k',\sigma'} \right) + h.c. \right] \end{aligned} \quad (19)$$

describes the dynamics of the data bus, where

$$\begin{aligned} A(k,k') &= e^{-i(k-k')\frac{l_0+1}{2}} \left[1 + e^{i(\theta_k - \theta_{k'})} \right], \\ B(k,k') &= e^{-i(k-k')\frac{l_0+1}{2}} \left[1 - e^{i(\theta_k - \theta_{k'})} \right]. \end{aligned} \quad (20)$$

Straightforward calculation shows that, in the thermodynamic limit, $N \rightarrow \infty$, the hopping constant becomes

$$g_{eff} = \frac{g^2}{g_0} \frac{(-1)^{\frac{l-1}{2}}}{1+\delta} \left(\frac{1-\delta}{1+\delta} \right)^{\frac{l-1}{2}}. \quad (21)$$

Here, we have used the one-dimensional integral to replace the discrete sum as $(2/N) \sum_k \rightarrow \int_0^{2\pi} dk/2\pi$.

It needs to be pointed out that the effective Hamiltonian H_{AB} works well only in the half-filled case. When the lower quasi-band is filled fully, the next excitation should jump over the gap and then virtual excitations can effectively induce the effective coupling. To demonstrate the above result about the effective long range hopping induced by the SSH chain, we schematically sketch the virtual process in Fig. 3, where the quanta of data bus between the two sites are exchanged. If the energy gap of the PDTBC is much larger than the connection couplings, $\Delta \gg g$, the virtual transition is essentially second order process. There are two kinds of virtual process for an initially half-filled state of the PDTBC. The first one happens via the exchange of the electron in the upper quasi-band, while the second one is based on the exchange of the hole in the lower quasi-band. We would

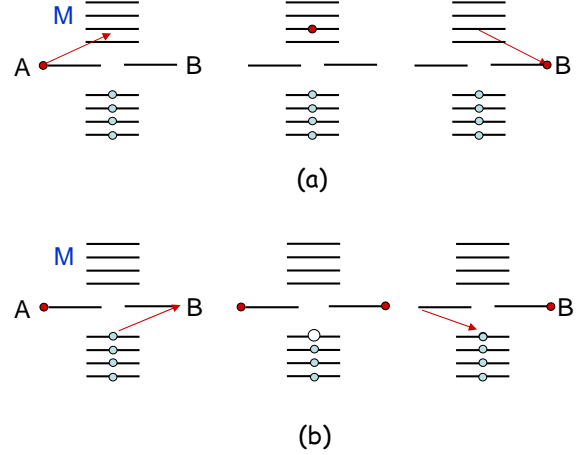


FIG. 3: Schematic illustration for the two processes of the second order perturbation. The virtual transitions of (a) electrons between $A(B)$ and the upper quasi-band and (b) holes between lower quasi-band and $A(B)$. These processes lead to effective hopping of electron between A and B directly.

like to remind that the two quasi-bands will become continuous in the thermodynamic limit. Nevertheless, there still exists indirect interaction between A and B as the effective results of the second order process.

Now we consider the scheme using the SSH chain to transfer the quantum state via the above effective virtual excitation process. Let Alice hold an electron with spin state

$$|\varphi\rangle = \cos \frac{\theta}{2} |\downarrow\rangle + e^{i\phi} \sin \frac{\theta}{2} |\uparrow\rangle \quad (22)$$

at the site A , where $|\uparrow\rangle$ ($|\downarrow\rangle$) denotes the spin up (down) state. Thus, the initial state $|\Psi(0)\rangle = |\varphi\rangle_A \otimes |0\rangle_B$ of the total system is

$$|\Psi(0)\rangle = \left(\cos \frac{\theta}{2} c_{A,\downarrow}^{\dagger} + e^{i\phi} \sin \frac{\theta}{2} c_{A,\uparrow}^{\dagger} \right) |0\rangle_{AB}.$$

Here, $|0\rangle_A$ ($|0\rangle_{AB}$) denotes the empty state, i.e., there is no electron at site A (both sites A and B). At the instant

$$t = \tau = \frac{\pi}{2|g_{eff}|}, \quad (23)$$

the total system evolves into a new factorized state $|\Psi(\tau)\rangle = |0\rangle_A \otimes |\varphi\rangle_B$ or

$$|\Psi(\tau)\rangle = \left(\cos \frac{\theta}{2} c_{B,\downarrow}^{\dagger} + e^{i\phi} \sin \frac{\theta}{2} c_{B,\uparrow}^{\dagger} \right) |0\rangle_{AB},$$

to realize a perfect quantum swapping. Then Bob at the site B can receive an electron with spin state $|\varphi\rangle$. Here, τ determines the characteristic time of quantum state transfer between two locations A and B , so the

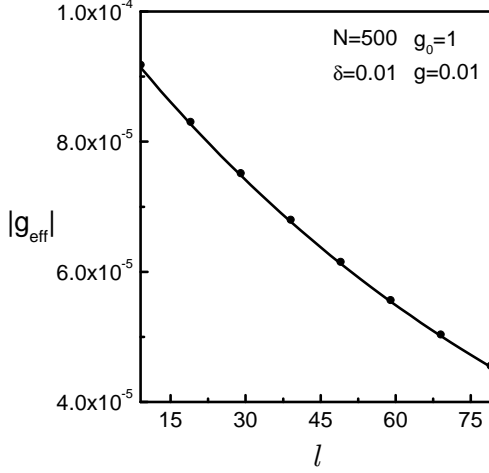


FIG. 4: The magnitude of effective hopping integral g_{eff} for the finite systems obtained by numerical exact diagonalization (solid dot) and the approximate analytical results from Eq. 21 (line). Here only odd l is plotted. It shows that g_{eff} decays not so fast in this range of l and the exact numerical and approximate analytical results are in agreement with each other very well.

behavior of $|g_{eff}|$ vs. l is crucial for quantum information transfer.

It is desirable that the above scheme for QST based on the SSH virtual excitation can work well over a longer distance, namely, the effective hopping integral g_{eff} should not decay too fast as the distance of two points AB increases. According to Eq. (21), $|g_{eff}|$ decays exponentially as l increases. However, $\sqrt{(1-\delta)/(1+\delta)}$ closes to 1 for small δ . So $|g_{eff}|$ does not decay rapidly for any finite l . To demonstrate this, numerical simulation is performed. The value of $|g_{eff}|$ is computed from the energy spacing between the ground and first excited states of the total system by exact diagonalization method for the finite system with $N = 500$, $l = 10n + 9$, $n \in [0, 7]$, $\delta = 0.01$, $g = 0.01$, and $g_0 = 1.0$. The exact numerical result and the analytical result obtained from Eq. (21) are plotted in Fig. 4. It shows that they are in agreement with each other well and $|g_{eff}|$ exhibits power law decay for finite l . It indicates that the characteristic time τ is proportional to the distance l , which is crucial for the scalable quantum information processing.

IV. REDUCED DENSITY MATRIX AND ENTANGLEMENT

In the above section, we studied the behavior of $|g_{eff}|$ changing as the distance l increases. It determines the speed of the QST via this SSH chain. However, all the conclusions obtained should be based on the fact that the effective Hamiltonian H_{AB} given by (17) is valid. In this section, we investigate the validity of the effective Hamil-

tonian H_{AB} by comparing the eigenstates of H_{AB} with the density matrix reduced from the ground and first excited states of the total system (11). Notice that the Hamiltonian (11) does not contain the spin-spin interaction term. Then we can regard the system as a spinless fermion system and then apply the result obtained feasibly for the spinless case to the original system. Therefore, in the following discussion we will ignore the spin degree of freedom for simplicity.

We define the states $|n_-, n_+\rangle_{AB}$ by

$$\begin{aligned} |1, 0\rangle_{AB} &= \frac{1}{\sqrt{2}} (a_A^\dagger - a_B^\dagger) |0\rangle_{AB}, \\ |0, 1\rangle_{AB} &= \frac{1}{\sqrt{2}} (a_A^\dagger + a_B^\dagger) |0\rangle_{AB} \end{aligned} \quad (24)$$

to denote the eigenstates of H_{AB} in the half-filled subspace, where a_A^\dagger, a_B^\dagger are spinless fermion operator at sites A and B . Here, n_- (n_+) is the number of particles in the anti-bonding (bonding) state. Then we calculate the “fidelity” of eigenstate defined by $P_{n_-, n_+} = \text{Tr}(\rho_R \rho_{n_-, n_+})$ or

$$P_{n_-, n_+} = \sum_{\eta} |\langle n_-, n_+ | n_-, n_+, \eta \rangle_{AB}|^2. \quad (25)$$

Obviously, it can be described as the expectation value of the effective density matrix $\rho_{n_-, n_+} = |n_-, n_+\rangle_{AB} \langle n_-, n_+|$ in the exact eigenstates $|n_-, n_+, \eta\rangle$ of the total system with the reduced density matrix $\rho_R = \text{Tr}_{SSH}(|n_-, n_+\rangle \langle n_-, n_+|)$. Here, $|n_-, n_+, \eta\rangle = |n_-, n_+\rangle_{AB} |\eta\rangle_{SSH}$ denotes the eigenstates of (11) with $g = 0$, while $|\eta\rangle_{SSH}$ denotes the groundstate ($\eta = 0$) and excited eigenstates ($\eta = 1, 2, \dots$) of the half-filled SSH chain. State $|n_-, n_+\rangle$ is the ground or first excited states of the whole system (the Hamiltonian (11) with $g \neq 0$), which are spanned by the states possessing the same parity as the states $|n_-, n_+; 0\rangle = |n_-, n_+\rangle_{AB} \otimes |0\rangle_{SSH}$.

On the other hand, it is known that the eigenstates of H_{AB} with unity concurrence are maximally entangled states [16, 17]. Thus by calculating the mode concurrences of two sites A and B for the ground and first excited states of the total system (11), one can verify whether the exact solutions can be well approximated by that from the effective Hamiltonian. If “fidelities” or concurrences is near unity, it can be concluded that the effective Hamiltonian H_{AB} is indeed valid for the perfect QST.

In the following discussion, we try to explicitly express the exact eigenstates $|n_-, n_+\rangle$ of the total system with the help of the Gellmann-Low theorem [18]. In quantum field theory, this theorem is used successfully to obtain the ground state of the interaction field from the ground state of the free field. The exact eigenstates can be expressed with the “input field” $|n_-, n_+; 0\rangle$ as

$$|n_-, n_+\rangle = \frac{U(0, -T) |n_-, n_+; 0\rangle}{e^{-iE_{\pm 0}T} \langle n_-, n_+ | n_-, n_+; 0\rangle}, \quad (26)$$

for $T \rightarrow \infty (1 + i\epsilon)$. Here,

$$U(t, t_0) = \mathcal{T} \exp \left\{ -i \int_{t_0}^t dt' H_I'(t') \right\} \quad (27)$$

is the time-evolution operator in the interaction picture, where \mathcal{T} is the time-ordering symbol and $H_I'(t') = \exp(iH_{SSH}t')H_I \exp(-iH_{SSH}t')$. Similarly, we have the “output field”

$$\langle n_-, n_+ | = \frac{\langle n_-, n_+; 0 | U(T, 0)}{e^{-iE_{\pm 0}T} \langle n_-, n_+; 0 | n_-, n_+ \rangle}. \quad (28)$$

With these formal expressions for the exact eigenstates of the total system, we can calculate reduced density matrix with respect to the AB -subsystem. Then the expectation value of the projection operators of $|n_-, n_+\rangle_{AB}$ in $|n_-, n_+\rangle$ can be calculated as

$$P_{n_-, n_+} = \frac{\langle n_-, n_+; 0 | Q | n_-, n_+; 0 \rangle}{e^{-iE_{\pm 0}(2T)} |\langle n_-, n_+; 0 | n_-, n_+ \rangle|^2}, \quad (29)$$

where

$$Q = \mathcal{T} \left\{ Q_{n_-, n_+} \exp \left[-i \int_{-T}^T dt' H_I'(t') \right] \right\}, \quad (30)$$

and

$$Q_{n_-, n_+} = |n_-, n_+\rangle_{AB} \langle n_-, n_+ | \otimes \mathbf{1}. \quad (31)$$

Notice that the above equation can not be calculated directly, because there is not an explicit expression for $|n_-, n_+\rangle$ with respect to the well known basis vectors $|n_-, n_+; 0\rangle$. To get rid of this difficulty, we use the normalization condition $\langle n_-, n_+ | n_-, n_+ \rangle = 1$ or

$$1 = \frac{\langle n_-, n_+; 0 | U(T, -T) | n_-, n_+; 0 \rangle}{e^{-iE_{\pm 0}(2T)} |\langle n_-, n_+; 0 | n_-, n_+ \rangle|^2}. \quad (32)$$

Then the Eq. (29) is rewritten as

$$P_{n_-, n_+} = \frac{\langle n_-, n_+; 0 | Q | n_-, n_+; 0 \rangle}{\langle n_-, n_+; 0 | U(T, -T) | n_-, n_+; 0 \rangle}. \quad (33)$$

If the connection between sites AB and SSH chain is switched off, i.e., the hopping integral in H_{AB} vanishes, states $|1, 0; 0\rangle$ and $|0, 1; 0\rangle$ are the eigenstates corresponding to vanishing eigen energies. Thus we can expand P_{n_-, n_+} , which equals to unity when H_{AB} is exact, as the series of g . The Dyson expansion of $U(T, -T)$ also gives the numerator and the denominator in the form of the series of g . Comparing the terms of each order with respect to small coupling g , the zero order of P_{n_-, n_+} ($P_{n_-, n_+}^{(0)}$) is unity, while the first order of P_{n_-, n_+} ($P_{n_-, n_+}^{(1)}$) is zero as a result of the particle number conservation, and second order of P_{n_-, n_+} ($P_{n_-, n_+}^{(2)}$) is non-zero and can be expressed as

$$P_{n_-, n_+}^{(2)} = - \sum_k \frac{2g^2}{\epsilon_k^2 N} \left[1 + (n_- - n_+) \cos \left(k \frac{l-1}{2} - \theta_k \right) \right]. \quad (34)$$

It approximately describes the difference between the eigenstates of H_{AB} and those reduced states from the exact eigenstates of the total system. In order to clearly characterize our model by the correction $P_{n_-, n_+}^{(2)}$, we have the upper bound of $P_{n_-, n_+}^{(2)}$ directly from (34) as

$$|P_{n_-, n_+}^{(2)}| \leq \frac{4}{N} \sum_k \frac{g^2}{\epsilon_k^2}. \quad (35)$$

In the thermodynamic limit, this upper bound becomes

$$|P_{n_-, n_+}^{(2)}| \leq \frac{g^2}{2g_0^2 \delta}. \quad (36)$$

This inequality provides us a necessary condition for the validity of the effective Hamiltonian H_{AB} . Actually, the necessary condition is $g^2/(2g_0^2 \delta) \ll 1$, which requires the validity condition

$$g/(\sqrt{2}g_0) \ll \sqrt{\delta}. \quad (37)$$

On the other hand, the sufficient condition is $g/g_0 \ll 1$ for this scheme. Then, if we take $\delta = g/g_0 \ll 1$, it should satisfy the sufficient and necessary conditions under which the effective Hamiltonian can work well.

In this paper, we take $\delta = g/g_0 = 0.01$ for the numerical calculation to demonstrate the validity of this scheme. Furthermore, the behavior of P_{n_-, n_+} around the point $\delta = 0$, in which region the above condition (37) is violated, is also investigated by numerical method. It shows that P_{n_-, n_+} deviate from unity within this region. We will discuss this problem in detail in the following.

Moreover, the mode concurrence between A and B for the state $|n_-, n_+\rangle$ can be gained from P_{n_-, n_+} . It could also be used to characterize the validity of the effective Hamiltonian H_{AB} . The mode concurrence for the state $|n_-, n_+\rangle$ is

$$C_{n_-, n_+} = \max \left\{ 0, \langle X \rangle_{n_-, n_+} + 2 \left| \langle Y \rangle_{n_-, n_+} \right| - 1 \right\}, \quad (38)$$

where $X = n_A + n_B - 2n_{AB}$, $Y = a_A^\dagger a_B + a_B^\dagger a_A$, and $\langle O \rangle_{n_-, n_+} = \langle n_-, n_+ | O | n_-, n_+ \rangle$ denotes the average value for an arbitrary operator O ([19]). Since states $|n_-, n_+\rangle$ and $|n_-, n_+\rangle_{AB} \otimes |0\rangle$, possess the same symmetry with respect to the points A and B , we have

$$\langle X \rangle_{n_-, n_+} + 2 \left| \langle Y \rangle_{n_-, n_+} \right| = \langle X - 2(n_- - n_+)Y \rangle_{n_-, n_+}. \quad (39)$$

Similarly, we have

$$Q_{n_-, n_+} = \frac{1}{2} [X - 2(n_- - n_+)Y] \quad (40)$$

Under the validity condition (37), P_{n_-, n_+} is near unity and $2P_{n_-, n_+} - 1$ should be larger than zero. So we have mode entanglement

$$C_{n_-, n_+} = 2P_{n_-, n_+} - 1. \quad (41)$$

l	$1 - P_{10}$ ($\times 10^{-3}$)	$P_{10}^{(2)}$ ($\times 10^{-3}$)	$1 - P_{01}$ ($\times 10^{-3}$)	$P_{01}^{(2)}$ ($\times 10^{-3}$)
9	4.48	4.53	5.39	5.38
19	0.41	0.41	0.46	0.47
29	4.66	4.70	3.69	3.68
39	0.38	0.38	0.46	0.47
49	4.60	4.64	4.30	4.30
59	0.50	0.50	0.45	0.46
69	4.45	4.49	5.80	5.80
79	0.67	0.67	0.44	0.44

TABLE I: P_{10} and P_{01} for the finite system with $N = 500$, $l = 10n + 9$, $n \in [0, 7]$, $\delta = 0.01$, $g = 0.01$, and $g_0 = 1.0$ obtained by numerical exact diagonalization and from the approximately analytical expression Eq. (34). They are in agreement with each other very well, which shows that the effective Hamiltonian H_{AB} can well describe the states of points A and B in the ground and first excited states of the total system.

Obviously, when the effective Hamiltonian H_{AB} is valid, the sites A and B are maximally entangled for the ground and first excited states of the whole system.

From the Eq. (21) about effective hopping integral g_{eff} , one can see that when $l = 4n + 1$ ($n = 0, 1, 2, \dots$), $|1, 0\rangle$ is the ground state of the total system, while $|0, 1\rangle$ is the ground state for $l = 4n + 3$, due to the sign of g_{eff} being positive or negative. We denote the expectation value P_{n-n+} of the projection operator for the ground and first excited states as P_g and P_e , respectively.

To demonstrate the validity of the effective Hamiltonian of the sites AB , numerical simulation is performed for the finite system. We calculate P_g and P_e for the finite system with $N = 500$, $l = 10n + 9$, $n \in [0, 7]$, $\delta = 0.01$, $g = 0.01$, and $g_0 = 1.0$ by numerical exact diagonalization and from the approximately analytical expression Eq. (34). The results are listed in Table 1. It shows that they are in agreement well and the single-particle (half-filled) eigenstates of the effective Hamiltonian H_{AB} can well describe the states of points A and B in the ground and first excited state of the total system. So H_{AB} is valid when temperature $T \ll 4g_0\delta/k_B$.

In the above studies, it is found that the magnitude of distortion δ is crucial for the quantum data bus to perform QST and the speed of QST is sensitive to the dimerization. There are two types of dimerization corresponding to $\pm|\delta|$. It is interesting to investigate what happens near the transition point $\delta = 0$. In this region the analytical results obtained above is no longer valid due to the vanishment of the gap. Numerical simulation should be employed to calculate g_{eff} , P_g and P_e , which characterize the property of QST. The numerical results obtained by exact diagonalization for the systems with $N = 100, 200$, $l = 23, 33, 43$ is plotted in Fig. 5. It shows that when the systems approach to the critical point $\delta = 0$, the gap ΔE between the ground and first

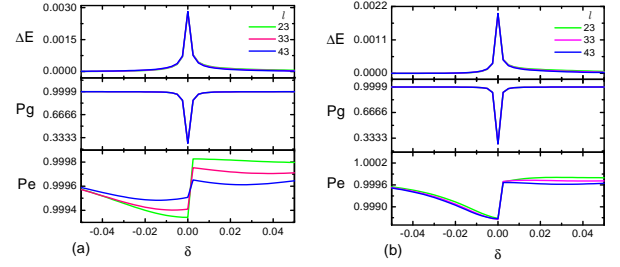


FIG. 5: The energy gap ΔE between the ground and first excited states, P_g , and P_e of the system with (a) $N = 100$; (b) $N = 200$, and $l = 23, 33, 43$, obtained by numerical exact diagonalization as the function of δ . When δ approaches to zero, the gap ΔE has a sharp peak, while P_g tends to 0.25, P_e remains unitary approximately. It shows that although QST becomes fast, the fidelity decreases rapidly around $\delta = 0$. This observation indicates that the features of two sites A and B reveals the transition of the data bus.

excited states has a sharp peak, while P_g tends to 0.25, P_e remains unitary approximately with only a very slight jump around the transition point. It indicates that although QST becomes fast around the critical point, the fidelity decreases rapidly. This phenomenon is very similar to that discovered by Ref. [20]. This fact also implies that the features of two probing sites A and B , such as the fidelity (mode concurrence) and the recurrent time $\pi/\Delta E$, reveal the intrinsic nature of the quantum data bus, a quantum phase transition-like behavior of the SSH chain.

V. QUANTUM DECOHERENCE BY PHONON EXCITATIONS

Finally we consider the decoherence problem due to the couplings with auxiliary modes concerning phonon excitations. To this end, we need to calculate the effect of electron-vibration coupling in the conducting polymers, which is off-resonate to the electron motion. The electron-vibration coupling gives rise to the disadvantage of the QST scheme based on SSH chain, though it does not dissipate the energy of the electronic subsystem.

Now we revisit the role of the electron-vibration coupling Hamiltonian (1) in the process of quantum information transfer based on the virtual excitation of the SSH model. We notice that there is no direct interaction between the electron motion and the quasi-excitation of SSH model when the energy gap is much larger than the connection couplings since $[H_{AB}, H_0] = 0$. Thus the main source of decoherence is due to electron-phonon couplings. This will realize a typical quantum decoherence model for a two level system coupled to a bath of harmonic oscillators [4, 22].

In order to analyze this decoherence problem more quantitatively, we describe the single mode phonon by

the perturbation

$$\delta = \gamma (b^\dagger + b), \quad (42)$$

induced by the quantized vibration of the SSH chain, where γ is a constant and b^\dagger (b) is the bosonic creation (annihilation) operator of the phonon excitation. In small distortion case, according to (21) the effective Hamiltonian depends on the phonon excitation through

$$g_{eff} \sim \omega_s [1 - l\gamma (b^\dagger + b)] \quad (43)$$

where

$$\omega_s = (-1)^{\frac{l-1}{2}} \frac{g^2}{g_0}. \quad (44)$$

Then we can rewrite the total Hamiltonian $H_D = H_q + H_P + H_{q-P}$ describing the quantum decoherence problem with

$$\begin{aligned} H_q &= \omega_s \sigma_x, \\ H_P &= \omega_0 b^\dagger b, \\ H_{q-P} &= -l\omega_s \gamma (b^\dagger + b) \sigma_x, \end{aligned} \quad (45)$$

where the Hamiltonian $H_q + H_{q-P}$ corresponds to H_{AB} and has been rewritten in terms of the quasi-spin operators

$$\begin{aligned} \sigma_x &= a_A^\dagger a_B + a_B^\dagger a_A, \\ \sigma_y &= -ia_A^\dagger a_B + ia_B^\dagger a_A, \\ \sigma_z &= a_A^\dagger a_A - a_B^\dagger a_B. \end{aligned} \quad (46)$$

Here, we have ignored the indices of the spin degree of freedom for avoiding confusion, because all results we obtain in the following are unrelated to spin.

Obviously, the effective electron-phonon coupling H_{q-P} can only lead to a phase shift in the spin qubit initially prepared in the quasi-spin states

$$|\rightarrow\rangle = |0, 1\rangle_{AB}, \quad |\leftarrow\rangle = |1, 0\rangle_{AB}. \quad (47)$$

It is also pointed out that the ground state (an eigenstate of the quasi-spin σ_x) of the effective Hamiltonian is a mode entanglement state. We consider the vibration mode initially prepared in a thermal equilibrium state

$$\rho_P = \frac{1}{Z} \sum_n e^{-\frac{\omega_0 n}{k_B T}} |n\rangle \langle n|, \quad (48)$$

at the temperature T , where the partition function is

$$Z = \frac{1}{1 - e^{-\frac{\omega_0}{k_B T}}}, \quad (49)$$

and k_B is the Boltzman constant.

Let the electron be initially in a pure state $|\phi\rangle = u|\rightarrow\rangle + v|\leftarrow\rangle$. After a straightforward calculation we get the density matrix at time t

$$\rho(t) = U(t) (|\phi\rangle \langle \phi| \otimes \rho_P) U^{-1}(t) \quad (50)$$

and the corresponding reduced density matrix $\rho_s(t) = \text{Tr}_P[\rho(t)]$ of AB can be obtained by tracing over the phonon modes. The off-diagonal elements of $\rho_s(t)$ can be given explicitly as

$$\rho_s^*(t)_{10} = \rho_s(t)_{01} = uv^* D(T, t), \quad (51)$$

where

$$D(T, t) = \exp \left[-\alpha^2 \sin^2 \left(\frac{\omega_0 t}{2} \right) \right], \quad (52)$$

is the so-called decoherence factor[4, 22]. The time independent factor

$$\alpha^2 = 2l^2 \left(\frac{2g^2\gamma}{g_0\omega_0} \right)^2 \coth \left(\frac{\omega_0}{2k_B T} \right) \quad (53)$$

depends on the temperature T and the distance l between A and B . The time dependent behavior of the decoherence factor is mainly determined by the oscillating factors $\sin^2(\omega_0 t/2)$. It indicates that, by increasing l and T , α^2 becomes larger. It leads to $D(T, t) \rightarrow 0$ except for some special instants at

$$t = \frac{2m\pi}{\omega_0}, m = 0, 1, 2, \dots \quad (54)$$

Here, $D(T, t)$ decays to a minimum $D_{\min} = \exp(-\alpha^2)$ as temperature increases. This result shows that thermal excitation of the phonons will block a perfect QST to some extent and this effect becomes prominent as the distance between A and B increases. To consider the extent of this influence about the QST scheme based on the SSH chain, we can calculate the fidelity or the purity $P = \text{Tr}_P[\rho_s(t) \rho_0(t)]$:

$$P = 1 + 2|uv^*|^2 [D(T, t) - 1] \quad (55)$$

with the ideal state

$$\rho_0(t) = e^{-iH_{AB}t} |\phi\rangle \langle \phi| e^{iH_{AB}t}. \quad (56)$$

The Eq. (55) shows the intrinsic relation between the purity and the decoherence factor.

Actually the off-diagonal elements are responsible for the intrinsic physics of QST, because the time evolution driven by H_{AB} for A and B will stop if off-diagonal elements vanish. We notice that the norms of off-diagonal elements is proportional to the decoherence factor $D(T, t)$. In order to show the influence of the electron-vibration coupling on the QST, 3D diagram of $D(T, t)$ is plotted in Fig. 6(a) for the case with $g_0 = 10^4 \omega_0$, $g = 10^2 \omega_0$, $\gamma = 10^{-2}$, $l = 9$, $t \in [0, 7\pi/\omega_0]$, and $T \in [k_B/4\omega_0, 10k_B/\omega_0]$. In Fig. 6(b) and (c), the cross sections of the 3D diagram for $D(T, t)$ are plotted to demonstrate the behavior of the decoherence factor. Actually, there exist other modes of phonon excitations in the SSH chain. But in the case of dimerization, the mode of phonon we described above dominates the quantum decoherence and thus it is reasonable that we only focus on the dimerization mode.

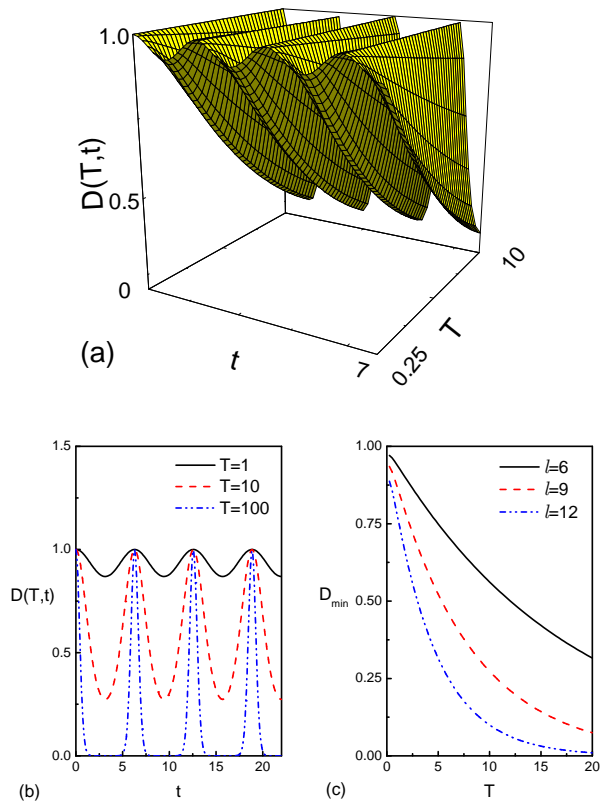


FIG. 6: (a) A 3D plot of the decoherence factor $D(T, t)$ as the function of the temperature and time for the case with $g_0 = 10^4 \omega_0$, $g = 10^2 \omega_0$, $\gamma = 10^{-2}$, $l = 9$, $t \in [0, 7\pi/\omega_0]$, and $T \in [k_B/4\omega_0, 10k_B/\omega_0]$. (b), (c) The cross section of $D(T, t)$ for different T and l . It shows that thermal excitation of the phonons will block a perfect QST as T or l increases.

VI. CONCLUSIONS

In this paper we proposed a QST scheme based on a desirable quantum data bus, which can be implemented by

a more practical system, the conducting polymers (polyacetylene) modeled as a SSH chain. This system serves as a quantum data bus with the following advantages. Firstly, the strength of the induced effective hopping of a qubit between two distant sites does not decay rapidly over the distance between them, and thus it can realize a fast quantum entanglement to transfer quantum information with the always-on coupling and minimal control. Secondly, there exists an energy gap to ensure the virtual excitation of the electrons in the SSH chain which induces the effective hopping of a qubit between two distant sites, but does not dissipate their energy. This shows the similar results to that of the spin ladder [10]. Thus a higher fidelity can be achieved for our QST scheme based on the virtual excitation of the SSH chain in lower temperature. Technologically, the more natural and less artificial designs with practical modulation about coupling constants for our protocol push the studies of QST based on real physical solid state system.

Furthermore, based on the analytical and numerical results, it is found that the validity of H_{AB} strongly depends on the distortion δ of the SSH chain. Thus, as a measurable issue, it essentially reflects the intrinsic property of the medium itself. In this sense, such a scheme can also be employed to explore the intrinsic property of the quantum system. These observations have some universality and may motivate us to investigate the functions of quantum data bus based on other real physical systems.

We acknowledge the support of the NSFC (grant No. 90203018, 10474104, 10447133), the Knowledge Innovation Program (KIP) of Chinese Academy of Sciences, the National Fundamental Research Program of China (No. 2001CB309310).

-
- [1] Michael A. Nielsen and Isaac L. Chuang, Quantum Computation and Quantum Information (Cambridge University Press, Cambridge, UK, 2001).
 - [2] S. M. Barnett, O Hirota, and E Andersson (Eds.), Quantum Communication, Measurement And Computing: The Seventh International Conference On Quantum Communication, Measurement And Computing International Conference on Quantum Comm, Springer Verlag (2004)
 - [3] M. D. Lukin, S. F. Yelin, and M. Fleischhauer, Phys. Rev. Lett **84**, 4232 (2000).
 - [4] C. P. Sun, Y. Li, and X. F. Liu, Phys. Rev. Lett **91**, 147903 (2004).
 - [5] C. H. Bennett, David P. DiVincenzo, Nature **404**, 247-255 (2000).
 - [6] S. Bose, Phys. Rev. Lett **91**, 207901 (2003).
 - [7] M. Christandl, N. Datta, A. Ekert and A. J. Landahl, Phys. Rev. Lett **92**, 187902 (2004).
 - [8] T. Shi, Y. Li, Z. Song and C. P. Sun, Phys. Rev. A **71**, 032309 (2005).
 - [9] S. Yang, Z. Song, and C.P. Sun, Phys. Rev. A **73**, 022317 (2006); S. Yang, Z. Song, and C.P. Sun, Phys. Rev. B **73**, 195122 (2006); S. Yang, Z. Song, and C.P. Sun quant-ph/062209.
 - [10] Ying Li, Tao Shi, Bing Chen, Zhi Song, and C.P. Sun, Phys. Rev. A **71**, 022301 (2005).
 - [11] W. P. Su, J. R. Schrieffer, and A. J. Heeger, Phys. Rev. Lett **42**, 1698 (1979); Phys. Rev. B **22**, 2099-2111 (1980).
 - [12] H. Fröhlich, Phys. Rev. **79**, 845 (1950).
 - [13] S. Nakajima, Adv. Phys. **4**, 363 (1953).

- [14] R.E. Peierls, Quantum Theory of Solids (Oxford, Univ. Press, London, 1955), p. 108.
- [15] L Yu, Solitons and Polarons in Conducting Polymers, World Scientific: Singapore, (1988).
- [16] W. K. Wootters, Phys. Rev. Lett **80**, 2245 (1998).
- [17] X. F. Qian, T. Shi, Y. Li, Z. Song and C. P. Sun, Phys. Rev. A **72**, 012333 (2005).
- [18] M. Gell-Mann and F. Low, Phys. Rev. **84**, 350 (1951).
- [19] X. F. Qian, Y. Li, Z. Song and C. P. Sun, Phys. Rev. A **72**, 062329 (2005).
- [20] M. J. Hartmann, M. E. Reuter, and Martin B. Plenio, quant-ph/0511185.
- [21] C.P. Sun, Phys. Rev. **A** 48, 898 (1993), in Quantum-Classical Correspondence, Ed. by D.H. Feng and B.L.Hu 99-106 (International Press,1994); in Quantum Coherence and Decoherence, Ed. by K. Fujikawa and Y.A.Ono, pp. 331-334, (Amsterdam: Elsevier Science Press,1996); C.P. Sun, X.X. Yi and X.J. Liu, Fortschr. Phys.**43**, 585 (1995).
- [22] Z. Song, P. Zhang, T. Shi, C. P. Su, Phys. Rev. **B** 71, 205314 (2005).